Adjustable Thermal Expansion Properties in $Zr_2MoP_2O_{12}$/ZrO_2 Ceramic Composites

Hongfei Liu[1], Weikang Sun[1], Xiang Xie[1], Lu Yang[1], Zhiping Zhang[2]*, Min Zhou[1], Xianghua Zeng[1] and Xiaobing Chen[2]

[1] Department of Microelectronics, School of Physical Science and Technology, Yangzhou University, Yangzhou, China,
[2] Department of Electrical and Mechanical Engineering, Guangling College, Yangzhou University, Yangzhou, China

$Zr_2MoP_2O_{12}$/ZrO_2 composites were successfully synthesized by the solid state method in attempt to fabricate the near-zero thermal expansion ceramics. The phase composition, micromorphology and thermal expansion behavior of the $Zr_2MoP_2O_{12}$/ZrO_2 composites with different mass ratios were investigated using X-ray diffraction, scanning electron microscopy and thermal mechanical analysis. Results indicate that $Zr_2MoP_2O_{12}$/ZrO_2 composites can be prepared by pre-sintering at 500°C for 3 h and then sintering at 1050°C for 6 h. The resulting $Zr_2MoP_2O_{12}$/ZrO_2 composites consisted of orthorhombic $Zr_2MoP_2O_{12}$ and monoclinic ZrO_2. With increasing content of $Zr_2MoP_2O_{12}$, the $Zr_2MoP_2O_{12}$/ZrO_2 ceramics became more compact and the coefficient of thermal expansion decreased gradually. $Zr_2MoP_2O_{12}$/ZrO_2 composites show an adjustable coefficient of thermal expansion (CTE) from 5.57×10^{-6} K^{-1} to -5.73×10^{-6} K^{-1} by changing the mass ratio of $Zr_2MoP_2O_{12}$ and ZrO_2. The $Zr_2MoP_2O_{12}$/ZrO_2 composite with a mass ratio of 2:1 showed near zero thermal expansion, and the average linear thermal expansion coefficient is measured to be 0.0065×10^{-6} K^{-1} in the temperature range from 25 to 700°C.

Keywords: ceramics, $Zr_2MoP_2O_{12}$, ZrO_2, composites, thermal expansion control

INTRODUCTION

It is well known that the vast majority of materials expand on heating. However, some materials shrink as the temperature rises and display negative thermal expansion (NTE). NTE materials have attracted considerable attention due to the anomalous phenomenon and their potential application in controlled thermal expansion composites and other areas (Chen et al., 2015). Control of thermal expansion is crucial to many applications. Mismatch of thermal expansion in component materials of high-precision device may result in serious problems, such as mechanical destruction and positional deviation. An easy method to prepare the material with near-zero or low thermal expansion is combining NTE materials with positive thermal expansion materials (Liu et al.2012; 2012a; Gao et al., 2016; Zhang et al., 2017). Materials displaying zero or low thermal expansion are both dimensionally stable and highly resistant to thermal shock.

The longtime leading NTE exemplar was ZrW_2O_8. Cubic ZrW_2O_8 exhibits strong isotropic NTE over a wide temperature range (Mary et al., 1996; Nishiiyama et al., 2006; Kanamori et al., 2008; Banek et al., 2010; Liu et al., 2011, 2012b). With the goal of thermal expansion control, several studies of the composites containing ZrW_2O_8 have been reported, such as ZrW_2O_8/ZrO_2 (Lommens et al., 2005; Yang et al., 2007), ZrW_2O_8/Cu (Yilmaz, 2002), ZrW_2O_8/Al (Wu et al., 2013), ZrW_2O_8/cement (Kofteros et al., 2001), ZrW_2O_8/PI, and ZrW_2O_8/epoxy (Sullivan and Lukehart, 2005; Yang et al., 2010). The thermal expansion coefficient of composites can be effectively controlled by using ZrW_2O_8 as NTE filler, however, the cubic ZrW_2O_8 is metastable at room temperature and needs to be quenched after sintering at 1200°C. Meanwhile, ZrW_2O_8 undergoes a structural phase transition from α-ZrW_2O_8 to β-ZrW_2O_8 at around 160°C and the coefficient of thermal expansion will decrease from about -8.8×10^{-6} K^{-1} to -4.9×10^{-6} K^{-1}. In addition, when ZrW_2O_8 was heated to about 740°C in air, it will decompose into ZrO_2 and WO_3 (Mary et al., 1996; Nishiiyama et al., 2006; Kanamori et al., 2008; Banek et al., 2010; Liu et al., 2011, 2012b). Quenching, thermal decomposition and the abrupt change of thermal expansion are disadvantageous for composite design.

Orthorhombic $Zr_2MoP_2O_{12}$, a member of $A_2M_3O_{12}$ family, has received widespread attention in recent years. It shows stable NTE and its average linear expansion coefficient is -4.5×10^{-6} K^{-1} over a broad temperature range from -264 to 1050°C. What's more, it overcomes all the limitations of ZrW_2O_8 discussed above, suggesting its potential use for fabricating near-zero or low thermal expansion materials (Cetinkol et al., 2009; Isobe et al., 2016). ZrO_2 ceramics has been widely used in optical, electrical and high temperature fields. The average linear thermal expansion coefficient of ZrO_2 is about 10×10^{-6} K^{-1}(Lommens et al., 2005; Yang et al., 2007). The absolute values of thermal expansion coefficient of ZrO_2 and $Zr_2MoP_2O_{12}$ are thus similar but have opposite signs, suggesting that these materials are good candidates for the preparation of ceramic composites with tunable CTEs. In this work, a new series of $Zr_2MoP_2O_{12}$/ZrO_2 composites were synthesized by solid state method with the goal of tailoring the thermal expansion. The effects of mass ratio between $Zr_2MoP_2O_{12}$ and ZrO_2 on the phase composition, microstructure, and thermal expansion coefficient of the $Zr_2MoP_2O_{12}$/ZrO_2 ceramic composites were also investigated.

EXPERIMENTAL

Sample Preparation

$Zr_2MoP_2O_{12}$, ZrO_2, and $Zr_2MoP_2O_{12}$/ZrO_2 composites (mass ratios: 1:2, 1:1, 2:1) were prepared using stoichiometric amounts of ZrO_2 (purity ≥99.95%, metals basis), MoO_3 (purity ≥99.99%, metals basis), and $NH_4H_2PO_4$ (purity ≥99.5%, metals basis). A summary of samples prepared can be found in **Table 1**. The starting compounds were mixed in ethanol using ball milling for 6 h to form a uniform mixture and dried at 80°C, then the mixtures were pre-heated at 500°C for 3 h. The mixtures, under 50 MPa, were cold pressed into pellets which were 7 mm in diameter and about 2 mm in thickness. Finally, the pellets were

TABLE 1 | Synthesis conditions for ZrO_2, $Zr_2MoP_2O_{12}$, and $Zr_2MoP_2O_{12}$/ZrO_2 ceramics.

Mass ratios of $Zr_2MoP_2O_{12}$:ZrO_2	m(ZrO_2)/g	m(MoO_3)/g	m($NH_4H_2PO_4$)/g
0:1	10	0	0
1:2	9.8523	1.0824	1.7290
1:1	8.7776	1.6227	2.5930
2:1	7.7038	2.1635	3.4576
1:0	4.1655	2.4330	3.8895

calcined at 1050°C in air for 6 h and cooled down in the furnace. In the solid-state synthesis, the following reactions may take place:

$$ZrO_2 + MoO_3 + 2NH_4H_2PO_4 \rightarrow ZrP_2O_7 + 2NH_3\uparrow$$
$$+ 3H_2O + MoO_3(500°C) \quad (1)$$
$$ZrO_2 + MoO_3 + ZrP_2O_7 \rightarrow Zr_2MoP_2O_{12}(1050°C) \quad (2)$$
$$Or:(1 + x)ZrO_2 + MoO_3 + ZrP_2O_7 \rightarrow Zr_2MoP_2O_{12}$$
$$+ xZrO_2(1050°C) \quad (3)$$
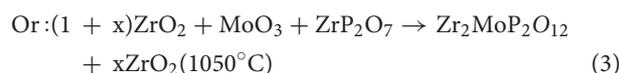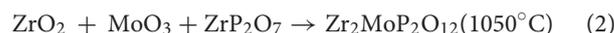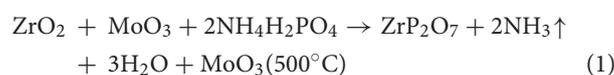
In this work, the 2:1 $Zr_2MoP_2O_{12}$/ZrO_2 composite was also prepared using the pure $Zr_2MoP_2O_{12}$ and ZrO_2 as raw materials, and the synthetic process is the same as that of the above process.

Experimental Techniques

Identification of the different phases presented in the samples was performed using powder X-ray diffraction (PXRD) on a Shimadzu XRD 7000 with Cu Ka radiation. Data were collected at 40 kV and 35 mA, with a scanning speed of 5°/min over an angular range of 10–60°. The micromorphologies of the samples were observed using a scanning electron microscopy (SEM, TESCAN VEGA3). The elemental composition of the samples were analyzed using energy-dispersive X-ray spectrometry (EDX, Bruker XFlash 6160) as well.The CTEs of the samples were measured by thermal mechanical analyzer (TMA/SS, Seiko 6300) using a heating rate of 5°C/min from room temperature to 700°C in air.

RESULTS AND DISCUSSION

XRD Analysis

Figure 1 shows typical XRD patterns of the $Zr_2MoP_2O_{12}$/ZrO_2 (mass ratios 1:2, 1:1, and 2:1) composites in addition to those of the pure $Zr_2MoP_2O_{12}$ and ZrO_2 ceramics obtained under the same preparation condition. **Figure 1a** shows typical powder XRD pattern of pure ZrO_2 ceramics sintered at 1050°C for 6 h, all the observed reflections could be well indexed and attributed to monoclinic ZrO_2 in agreement with JCPDS card number 65–1,023. The typical powder XRD pattern of pure $Zr_2MoP_2O_{12}$ specimen sintered at 1050°C for 6 h is shown in **Figure 1e**, all diffraction peaks match those expected for orthorhombic $Zr_2MoP_2O_{12}$, which agrees with literature reports (Cetinkol et al., 2009; Isobe et al., 2016). No impurity phases were detected, confirming the purity of the two products. The
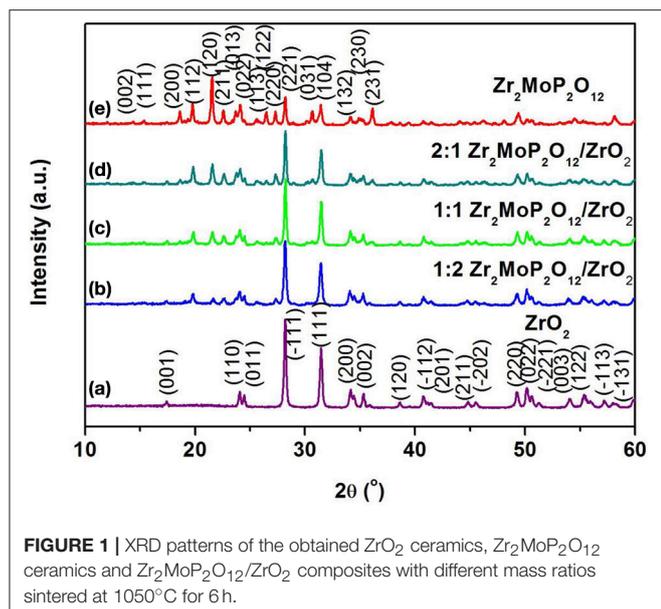
FIGURE 1 | XRD patterns of the obtained ZrO_2 ceramics, $Zr_2MoP_2O_{12}$ ceramics and $Zr_2MoP_2O_{12}$/ZrO_2 composites with different mass ratios sintered at 1050°C for 6 h.
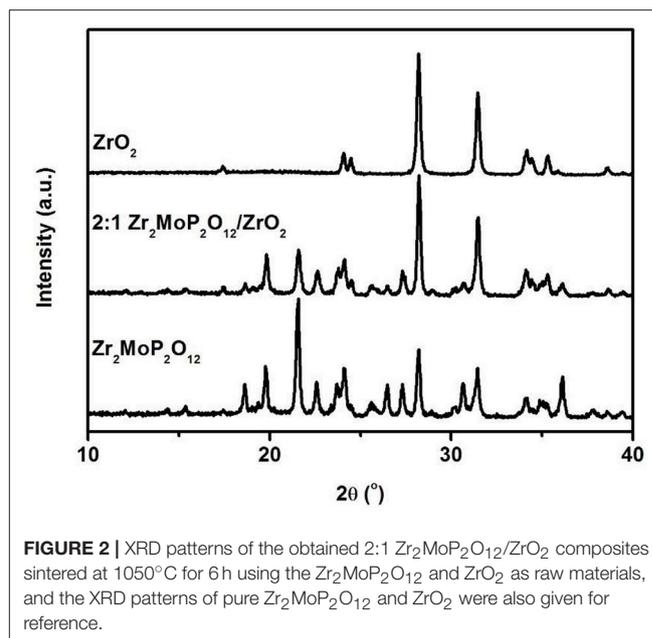
FIGURE 2 | XRD patterns of the obtained 2:1 $Zr_2MoP_2O_{12}$/ZrO_2 composites sintered at 1050°C for 6 h using the $Zr_2MoP_2O_{12}$ and ZrO_2 as raw materials, and the XRD patterns of pure $Zr_2MoP_2O_{12}$ and ZrO_2 were also given for reference.

PXRD patterns of the $Zr_2MoP_2O_{12}$/ZrO_2 (mass ratio: 1:2, 1:1, and 2:1) composites were shown in **Figures 1b–d**, it can be seen that all the diffraction peaks of the specimens could be indexed as both monoclinic ZrO_2 and orthorhombic $Zr_2MoP_2O_{12}$. With increasing mass ratio of $Zr_2MoP_2O_{12}$, the intensity of diffraction peaks of $Zr_2MoP_2O_{12}$ become much stronger. The diffraction peaks of both ZrO_2 and $Zr_2MoP_2O_{12}$ were sharp and intense, indicating their highly crystalline nature.

To investigate whether a chemical reaction occurred between ZrO_2 and $Zr_2MoP_2O_{12}$ during sintering at 1050°C. The 2:1 $Zr_2MoP_2O_{12}$/ZrO_2 composite was also prepared using the pure $Zr_2MoP_2O_{12}$ and ZrO_2 as raw materials. The $Zr_2MoP_2O_{12}$ was mixed with ZrO_2 at a mass ratio of 2:1 and finally calcined at 1050°C in air for 6 h. The XRD patterns of the ZrO_2, $Zr_2MoP_2O_{12}$, and 2:1 $Zr_2MoP_2O_{12}$/ZrO_2 were shown in **Figure 2**. Except for monoclinic ZrO_2 and orthorhombic $Zr_2MoP_2O_{12}$, no new peaks were detected, confirming that no chemical reaction occurred between ZrO_2 and $Zr_2MoP_2O_{12}$ during sintering at 1050°C.

SEM Images and Density Analysis

Further study was carried out by the SEM analysis to identify microstructures of as-prepared $Zr_2MoP_2O_{12}$, ZrO_2, and $Zr_2MoP_2O_{12}$/ZrO_2 composites. **Figure 3** shows SEM images of fracture surfaces of the pure ZrO_2, pure $Zr_2MoP_2O_{12}$ sintered bodies, and the $Zr_2MoP_2O_{12}$/ZrO_2 composites fabricated with different mass ratio of 1:2, 1:1, and 2:1. As shown in **Figure 3a**, as-prepared ZrO_2 ceramics sintered at 1050°C is not compact and the ZrO_2 grain growth is not observed obviously due to the insufficient sintering. The SEM images of the $Zr_2MoP_2O_{12}$/ZrO_2 composites fabricated at different mass ratio of 1:2, 1:1, and 2:1 are shown in **Figures 3b–d**. It can be seen that the $Zr_2MoP_2O_{12}$/ZrO_2 composites show nearly the same SEM images of fracture surfaces, which consist of irregular grains and some pores. With increasing content of $Zr_2MoP_2O_{12}$,

$Zr_2MoP_2O_{12}$/ZrO_2 ceramics became denser and displayed larger particle sizes and less porosity, suggesting that the increase of $Zr_2MoP_2O_{12}$ slightly promoted the particle growth and increased the density of the $Zr_2MoP_2O_{12}$/ZrO_2 ceramics. **Figure 3e** shows the SEM images of fracture surfaces of the obtained pure $Zr_2MoP_2O_{12}$ ceramics. The $Zr_2MoP_2O_{12}$ sintered body was denser compared with the ZrO_2 ceramics fabricated at same sintering temperature. It is compact, which is in agreement with the results reported earlier (Cetinkol et al., 2009; Isobe et al., 2016). The elemental composition and distribution of 2:1 $Zr_2MoP_2O_{12}$/ZrO_2 composite was also investigated using the EDX. The distribution of zirconium, oxygen, phosphorus, molybdenum is shown in **Figures 3f–j**.

Thermal Expansion Properties

For a better analysis of the thermal expansion behaviors of the composites, **Figure 4A** shows the thermal expansion curves of the $Zr_2MoP_2O_{12}$/ZrO_2 composites with different mass ratio calcined at 1050°C for 6 h. The thermal expansion curves of the pure $Zr_2MoP_2O_{12}$ and pure ZrO_2 ceramics are also given for reference. As shown in **Figures 4A-a**, Pure ZrO_2 specimen shows positive thermal expansion in the testing temperature from 25 to 700°C with an average linear thermal expansion coefficient of 5.57×10^{-6} K^{-1}, which agrees with literature reports (Lommens et al., 2005; Yang et al., 2007). In **Figures 4A-e**, it can be seen that pure $Zr_2MoP_2O_{12}$ ceramics showed strong negative thermal expansion. Its average linear thermal expansion coefficient was measured to be -5.73×10^{-6} K^{-1} in the testing temperature range of 25–700°C. It can be found that the thermal expansion curves of the obtained samples except pure $Zr_2MoP_2O_{12}$ ceramics overlap below 200°C, this abnormal behavior in the beginning of thermal expansion curves may be caused by the instrument. Above 200°C, all the samples show stable and almost linear change in the curves
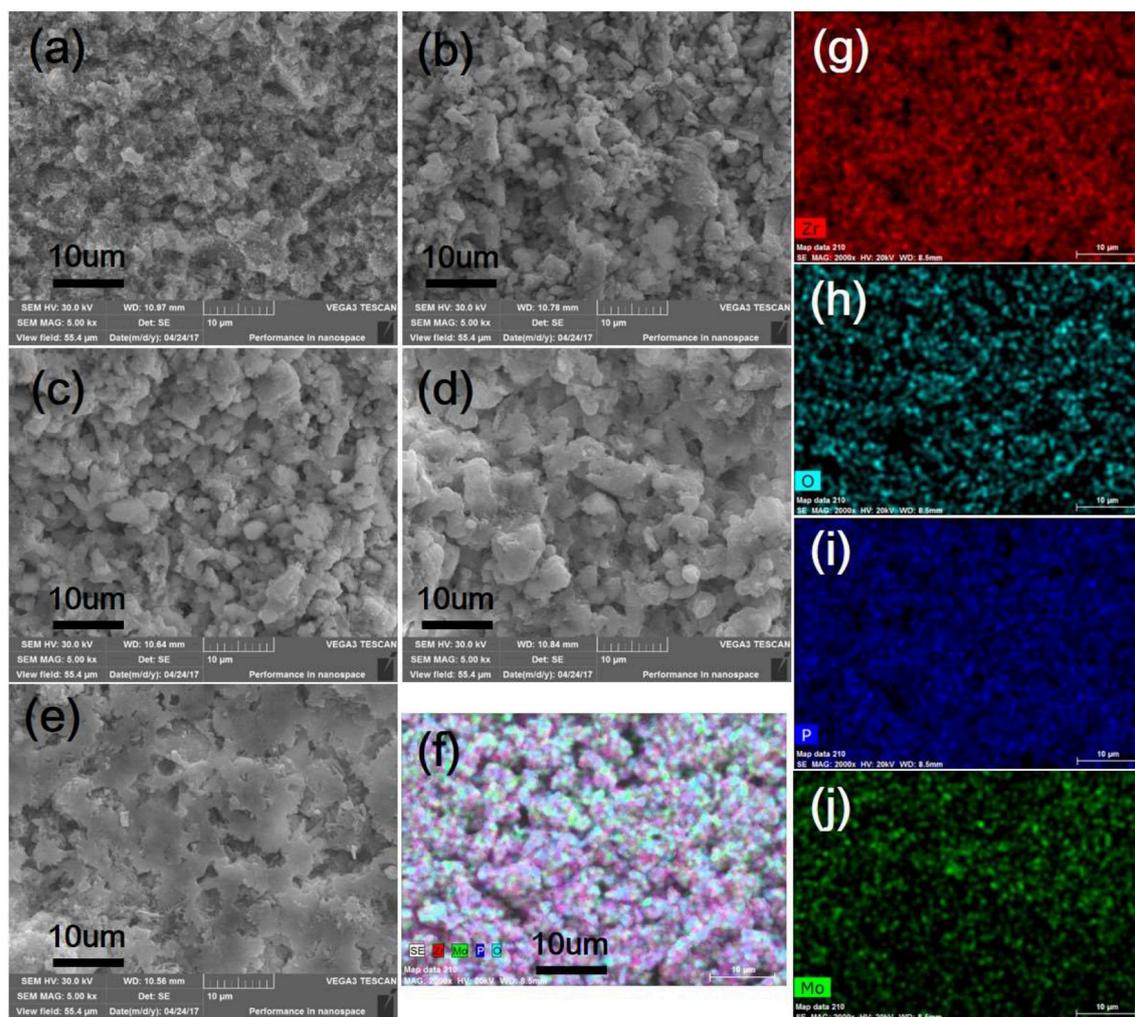
FIGURE 3 | SEM images of the obtained ZrO_2 ceramics, $Zr_2MoP_2O_{12}$ ceramics and $Zr_2MoP_2O_{12}/ZrO_2$ composites with different mass ratios sintered at 1050°C for 6 h. **(a)** ZrO_2 **(b)** $Zr_2MoP_2O_{12}$:ZrO_2 = 1:2 **(c)** $Zr_2MoP_2O_{12}$:ZrO_2 = 1:1 **(d)** $Zr_2MoP_2O_{12}$:ZrO_2 = 2:1 **(e)** $Zr_2MoP_2O_{12}$ **(f)** overlaid with elemental analysis results of 2:1 $Zr_2MoP_2O_{12}/ZrO_2$ composite using EDX **(g–j)** distribution of zirconium, oxygen, phosphorus, molybdenum elements in the selected area.

of thermal expansion with the increased temperature. Based on the above SEM analysis, the compact microstructure of the composites will promotes the stability of thermal expansion performance. Average linear thermal expansion coefficients of the obtained pure ZrO_2, pure $Zr_2MoP_2O_{12}$, and $Zr_2MoP_2O_{12}/ZrO_2$ composites with different mass ratios are summarized in **Table 2**. With increasing content of $Zr_2MoP_2O_{12}$, the thermal expansion coefficient of $Zr_2MoP_2O_{12}/ZrO_2$ composite decreased gradually. The 1:2 $Zr_2MoP_2O_{12}/ZrO_2$ composite showed positive thermal expansion with a thermal expansion coefficient of 2.30×10^{-6} K^{-1}. When the mass ratio of $Zr_2MoP_2O_{12}/ZrO_2$ decreased to 1:1, the composite also exhibited positive thermal expansion, but the CTE value decreased to 1.14×10^{-6} K^{-1}. The 2:1 $Zr_2MoP_2O_{12}/ZrO_2$ composite showed very low thermal expansion with an average linear thermal expansion coefficient of 0.0082×10^{-6} K^{-1} in the temperature range of 25–700°C. **Figure 4B** shows the cyclic thermal expansion curves of the

$Zr_2MoP_2O_{12}/ZrO_2$ composites. The two thermal expansion curves are almost the same, and the second average linear thermal expansion coefficient was test to be 0.0049×10^{-6} K^{-1} in the same temperature range, indicating the 2:1 $Zr_2MoP_2O_{12}/ZrO_2$ composite shows a stable thermal expansion property and the mass ratio of 2:1 ($Zr_2MoP_2O_{12}/ZrO_2$) is appropriate one. With the increase of the temperature, the volume shrinkage of the NTE $Zr_2MoP_2O_{12}$ just can accommodate the volume expansion of ZrO_2, which will keep a little change of the volume value of the 2:1 $Zr_2MoP_2O_{12}/ZrO_2$ composite. This near-zero expansion ceramic composite can withstand thermal stresses arising during sintering and subsequent quenching, which is an important criterion for a number of potential application in many fields. The results suggest that the thermal expansion coefficients of $Zr_2MoP_2O_{12}/ZrO_2$ composites can be tailored from 5.57×10^{-6} K^{-1} to -5.73×10^{-6} K^{-1} by adjusting the weight fraction of $Zr_2MoP_2O_{12}$. **Figure 5** shows the relation between coefficients of
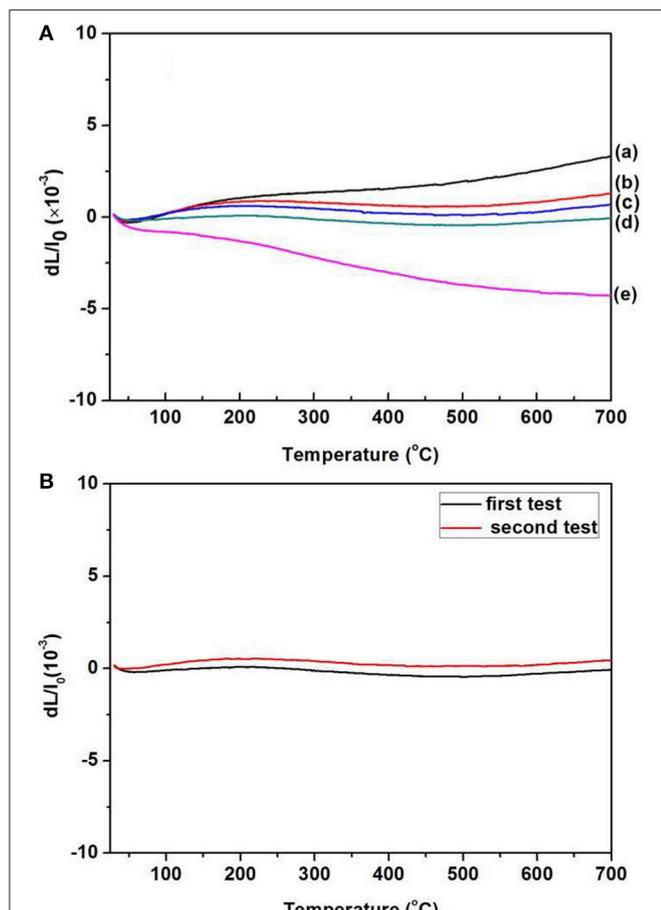
FIGURE 4 | (A) Thermal expansion curves of the obtained ZrO_2 ceramics, $Zr_2MoP_2O_{12}$ ceramics and $Zr_2MoP_2O_{12}/ZrO_2$ composites with different mass rati006Fs sintered at 1050°C for 6 h. **(a)** ZrO_2 **(b)** $Zr_2MoP_2O_{12}:ZrO_2$ = 1:2 **(c)** $Zr_2MoP_2O_{12}:ZrO_2$ = 1:1 **(d)** $Zr_2MoP_2O_{12}:ZrO_2$ = 2:1 **(e)** $Zr_2MoP_2O_{12}$. **(B)** Cyclic thermal expansion curves of the 2:1 $Zr_2MoP_2O_{12}/ZrO_2$ composite.

TABLE 2 | Average linear thermal expansion coefficients of ZrO_2 ceramics, $Zr_2MoP_2O_{12}$ ceramics, and $Zr_2MoP_2O_{12}/ZrO_2$ composites with different mass ratios in corresponding testing temperature range from 25 to 700°C.

Samples (mass ratio)	Coefficient of thermal expansion
ZrO_2	5.57×10^{-6} K^{-1}
$Zr_2MoP_2O_{12}/ZrO_2$ = 1:2	2.30×10^{-6} K^{-1}
$Zr_2MoP_2O_{12}/ZrO_2$ = 1:1	1.14×10^{-6} K^{-1}
$Zr_2MoP_2O_{12}/ZrO_2$ = 2:1	0.0065×10^{-6} K^{-1} (mean value)
$Zr_2MoP_2O_{12}$	-5.73×10^{-6} K^{-1}
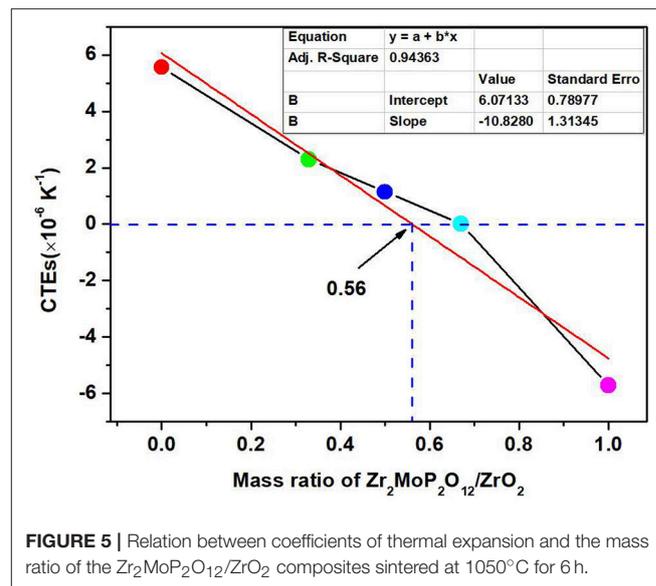
FIGURE 5 | Relation between coefficients of thermal expansion and the mass ratio of the $Zr_2MoP_2O_{12}/ZrO_2$ composites sintered at 1050°C for 6 h.

thermal expansion and the mass ratio of the $Zr_2MoP_2O_{12}/ZrO_2$ composites sintered at 1050°C for 6 h. The points is the data measured in the work. There is no linear relationship between the coefficients of thermal expansion and the mass ratio of the $Zr_2MoP_2O_{12}/ZrO_2$ composites. The red line is the best-fit line. According to the fitting equation, when the mass ration of $Zr_2MoP_2O_{12}/ZrO_2$ is 0.57, the $Zr_2MoP_2O_{12}/ZrO_2$ composite show zero thermal expansion. This fitting result deviates from the data obtained in the experiment. When the mass ration of $Zr_2MoP_2O_{12}/ZrO_2$ is 0.67, the near-zero thermal expansion $Zr_2MoP_2O_{12}/ZrO_2$ composite was obtained. This deviation mainly caused by the defects in the composites, such as pores and microcracks.

CONCLUSIONS

With the goal of thermal expansion control, NTE $Zr_2MoP_2O_{12}$ was combined with the positive thermal expansion ZrO_2 to

fabricate the composites with a tailorable thermal expansion. The obtained $Zr_2MoP_2O_{12}/ZrO_2$ composites synthesized at 1050°C for 6 h were composed of orthorhombic $Zr_2MoP_2O_{12}$ and monoclinic ZrO_2, no intermediate phase was observed. With increasing content of $Zr_2MoP_2O_{12}$, the thermal expansion coefficient of $Zr_2MoP_2O_{12}/ZrO_2$ composite decreased while the density of the composite increased gradually. The thermal expansion coefficients of the $Zr_2MoP_2O_{12}/ZrO_2$ composites can be tailored from 5.57×10^{-6} K^{-1} to -5.73×10^{-6} K^{-1} by changing the weight fraction of $Zr_2MoP_2O_{12}$. In addition, the 2:1 $Zr_2MoP_2O_{12}/ZrO_2$ composite displayed near-zero thermal expansion with an average linear thermal expansion coefficient of 0.0065×10^{-6} K^{-1} in the testing temperature range of 25–700°C. This near-zero thermal expansion material will have a number of potential application in many fields due to its dimensional stability and high resistance to thermal shock.

AUTHOR CONTRIBUTIONS

HL and ZZ designed experiments. WS, XX, and LY carried out experiments. HL, ZZ, XZ, MZ, and XC analyzed experimental results. HL and ZZ wrote the manuscript.

ACKNOWLEDGMENTS

REFERENCES

Banek, N. A., Baiz, H. I., Latigo, A., and Lind, C. (2010). Autohydration of nanosized cubic zirconium tungstate. *J. Am. Chem. Soc.* 132, 8278–8279. doi: 10.1021/ja101475f

Cetinkol, M., Wilkinson, A. P., and Lee, P. (2009). Structural changes accompanying negative thermal expansion in $Zr_2(MoO_4)(PO_4)_2$. *J. Solid State Chem.* 182, 1304–1311. doi: 10.1016/j.jssc.2009.02.029

Chen, J., Hu, L., Deng, J., and Xing, X. (2015). Negative thermal expansion in functional materials: controllable thermal expansion by chemical modifications. *Chem. Soc. Rev.* 44, 3522–3567. doi: 10.1039/C4CS00461B

Gao, X. D., Coleman, M. R., and Lind, C. (2016). Surface modification of ZrW_2O_8 and $ZrW_2O_7(OH)_2 \times 2H_2O$ filler particles for controlled thermal expansion polycarbonate composites. *Pol. Comp.* 37, 1359–1368. doi: 10.1002/pc.23304

Isobe, T., Houtsuki, N., Hayakawa, Y., Yoshida, K., Matsushita, S., and Nakajima, A. (2016). Preparation and properties of $Zr_2MoP_2O_{12}$ ceramics with negative thermal expansion. *Mater. Design.* 112, 11–16. doi: 10.1016/j.matdes.2016.09.048

Kanamori, K., Kineri, T., Fukuda, R., Nishio, K., and Yasumori, A. (2008). Preparation and formation mechanism of ZrW_2O_8 by Sol–Gel process. *J. Am. Ceram. Soc.* 90, 3542–3545. doi: 10.1111/j.1551-2916.2008.02726.x

Kofteros, M., Rodriguez, S., and Tandon, V. (2001). A preliminary study of thermal expansion compensation in cement by ZrW_2O_8 additions. *Scripta Mater.* 45, 369–374. doi: 10.1016/S1359-6462(01)01009-0

Liu, H. F., Zhang, W., Zhang, Z. P., and Chen, X. B. (2012a). Synthesis and negative thermal expansion properties of solid solutions $Yb_{2--x}La_xW_3O_{12}$ ($0 \leq x \leq 2$). *Ceram. Int.* 38, 2951–2956. doi: 10.1016/j.ceramint.2011.11.072

Liu, H. F., Zhang, Z. P., Zhang, W., and Chen, X. B. (2011). Negative thermal expansion ZrW_2O_8 thin films prepared by pulsed laser deposition. *Surf. Coat. Technol.* 205, 5073–5076. doi: 10.1016/j.surfcoat.2011.05.010

Liu, H. F., Zhang, Z. P., Zhang, W., and Chen, X. B. (2012b). Effects of HCl concentration on the growth and negative thermal expansion property of the ZrW_2O_8 nanorods. *Ceram. Int.* 38, 1341–1345. doi: 10.1016/j.ceramint.2011.09.010

Liu, Q. Q., Yang, J., Cheng, X. N., Liang, G. S., and Sun, X. J. (2012). Preparation and characterization of negative thermal expansion $Sc_2W_3O_{12}/Cu$ core–shell composite. *Ceram. Int.* 38, 541–545. doi: 10.1016/j.ceramint.2011.07.041

Lommens, P., Meyer, C. D., Bruneel, E., Buysser, K. D., Driessche, I. V., and Hoste, S. (2005). Synthesis and thermal expansion of ZrO_2/ZrW_2O_8 composites. *J. Europ. Ceram. Soc.* 25, 3605–3610. doi: 10.1016/j.jeurceramsoc.2004.09.015

Mary, T. A., Evans, J. S. O., Vogt, T., and Sleight, A. W. (1996). Negative thermal expansion from 0.3 K to 1050 K in ZrW_2O_8. *Science* 272, 90–92.

Nishiiyama, S., Hayashi, T., and Hattori, T. (2006). Synthesis of ZrW_2O_8 by quick cooling and measurement of negative thermal expansion of the sintered bodies. *J. Alloys Compd.* 417, 187–189. doi: 10.1016/j.jallcom.2005.07.075

Sullivan, L. M., and Lukehart, C. M. (2005). Zirconium tungstate (ZrW2O8)/polyimide nanocomposites exhibiting reduced coefficient of thermal expansion. *Chem. Mater.* 17, 2136–2141. doi: 10.1021/cm0482737

Wu, Y., Wang, M. L., Chen, Z., Ma, N. H., and Wang, H. W. (2013). The effect of phase transformation on the thermal expansion property in Al/ZrW_2O_8 composites. *J. Mater. Sci.* 48, 2928–2933. doi: 10.1007/s10853-012-6933-x

Yang, J., Yang, Y. S., Liu, Q. Q., Xu, G. F., and Cheng, X. N. (2010). Preparation of negative thermal expansion ZrW_2O_8 powders and its application in polyimide/ZrW_2O_8 composites. *J. Mater. Sci. Technol.* 26, 665–668. doi: 10.1016/S1005-0302(10)60103-X

Yang, X. B., Cheng, X. N., Yan, X. H., Yang, J., Fu, T. B., and Qiu, J. (2007). Synthesis of ZrO_2/ZrW_2O_8 composites with low thermal expansion. *Compos. Sci. Technol.* 67, 1167–1171. doi: 10.1016/j.compscitech.2006.05.012

Yilmaz, S. (2002). Thermal mismatch stress development in $Cu-ZrW_2O_8$ composite investigated by synchrotron X-ray diffraction. *Comp. Sci. Technol.* 62, 1835–1839. doi: 10.1016/S0266-3538(02)00104-5

Zhang, Z., Sun, W., Liu, H., Xie, G., Chen, X., and Zeng, X. (2017). Synthesis of $Zr_2WP_2O_{12}/ZrO_2$ composites with adjustable thermal expansion. *Front. Chem.* 5:105. doi: 10.3389/fchem.2017.00105